





Synthesis, structures, and magnetic properties of four dodecanuclear Ni_8RE_4 (RE = Gd, Dy, Y) clusters trapping four μ_5 -bridged carbonate anions

Hongshan Ke, Sheng Zhang, Wanxia Zhu, Gang Xie & Sanping Chen


To cite this article: Hongshan Ke, Sheng Zhang, Wanxia Zhu, Gang Xie & Sanping Chen (2015) Synthesis, structures, and magnetic properties of four dodecanuclear Ni_8RE_4 (RE = Gd, Dy, Y) clusters trapping four μ_5 -bridged carbonate anions, Journal of Coordination Chemistry, 68:5, 808-822, DOI: [10.1080/00958972.2015.1004326](https://doi.org/10.1080/00958972.2015.1004326)

To link to this article: <http://dx.doi.org/10.1080/00958972.2015.1004326>

 View supplementary material [↗](#)

 Accepted author version posted online: 07 Jan 2015.
Published online: 23 Jan 2015.

 Submit your article to this journal [↗](#)

 Article views: 74

 View related articles [↗](#)

 View Crossmark data [↗](#)

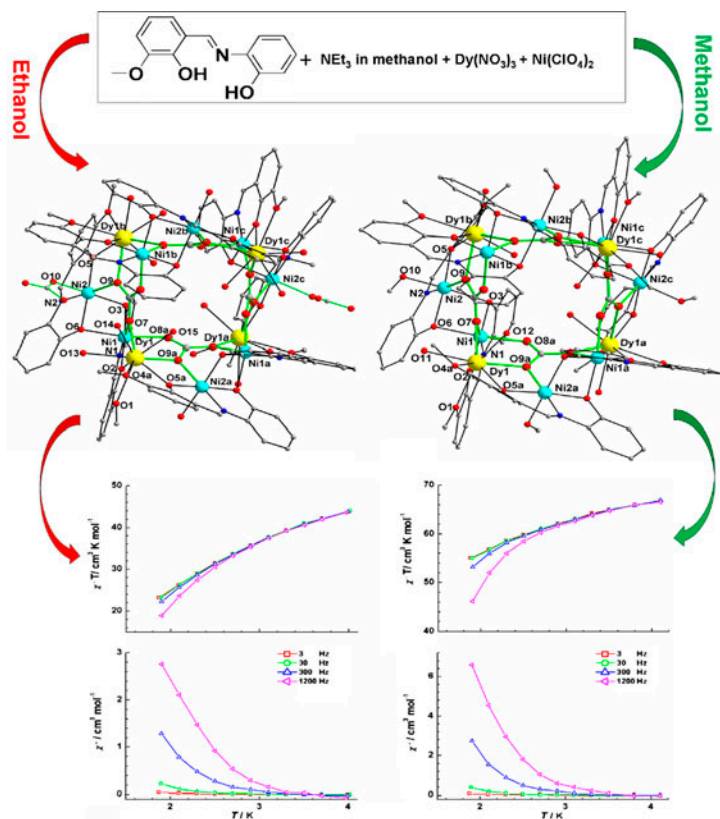
 Citing articles: 2 View citing articles [↗](#)

Synthesis, structures, and magnetic properties of four dodecanuclear Ni_8RE_4 (RE = Gd, Dy, Y) clusters trapping four μ_5 -bridged carbonate anions

HONGSHAN KE*, SHENG ZHANG, WANXIA ZHU, GANG XIE and SANPING CHEN

Key Laboratory of Synthetic and Natural Functional Molecule Chemistry of Ministry of Education, College of Chemistry and Materials Science, Northwest University, Xi'an, PR China

(Received 23 October 2014; accepted 29 December 2014)



*Corresponding author. Email: hske@nwu.edu.cn

By varying reaction solvent, four heterometallic dodecanuclear clusters trapping four μ_5 -bridged carbonates have been assembled. The Ni₈Dy₄ analogs display dissimilar static and dynamic magnetic behavior, which are ascribed to different coordination environments and ligand fields around the Dy^{III} ions.

The syntheses, structures, and magnetic properties of four heterometallic dodecanuclear aggregates with molecular formulas [Ni^{II}₈RE^{III}₄(L)₈(CO₃)₆(H₂O)₁₄·mCH₃OH·12H₂O [RE = Gd (**1**), *m* = 2; Dy (**2**), *m* = 0] and [Ni^{II}₈RE^{III}₄(L)₈(CO₃)₄(CH₃OH)₄(H₂O)₈]·(ClO₄)₄·8H₂O [RE = Dy (**3**), Y (**4**)] are presented. These complexes were obtained from two easy synthetic procedures through atmospheric CO₂ fixation involving direct reaction of 2-(2-hydroxy-3-methoxybenzylideneamino)phenol (H₂L) with RE(NO₃)₃·nH₂O and Ni(ClO₄)₂·6H₂O in the presence of triethylamine in different solvents under ambient conditions. Single-crystal X-ray diffraction reveals that these complexes possess very similar core structures featuring an unprecedented “tetra-capped hexahedron” topology bridged by four μ_5 -bridged carbonates. Static magnetic susceptibility measurements indicate dominant ferromagnetic coupling between the metal centers for **1** and **4**. The dissimilar static and dynamic magnetic behaviors seen in **2** and **3** are probably ascribed to different coordination environments and ligand fields around Dy^{III} ions. These complexes represent limited examples of high-nuclearity Ni^{II}-RE^{III} family trapping μ_5 -bridged carbonates through atmospheric carbon dioxide fixation.

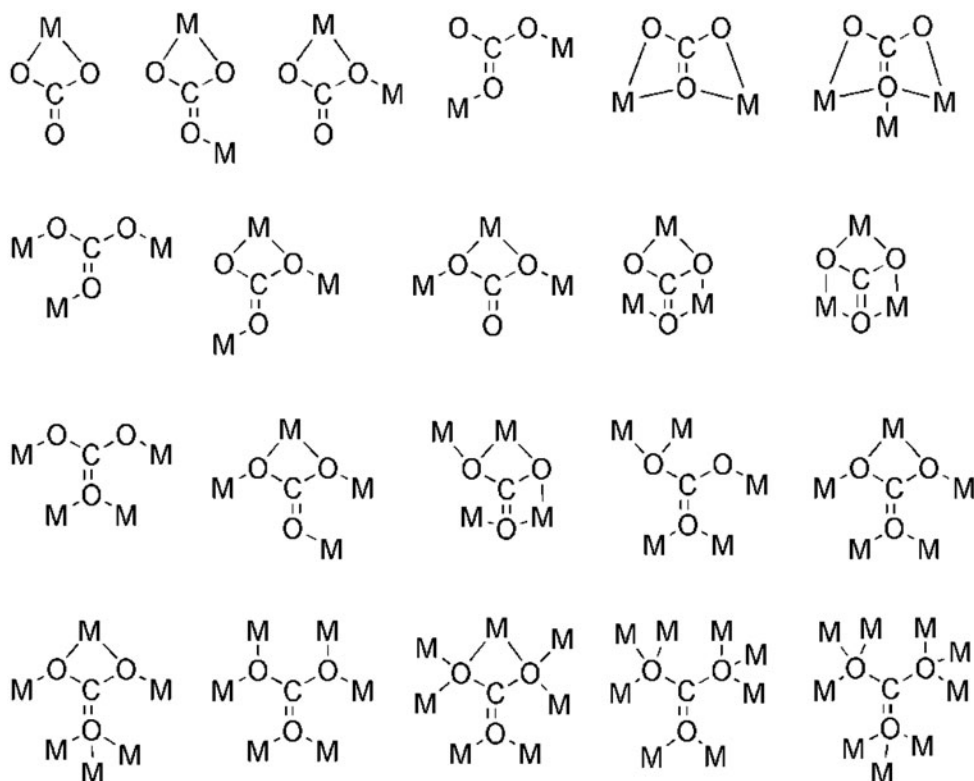
Keywords: Carbon dioxide fixation; Solvent effect; Heterometallic; Coordination perturbation; High nuclearity

1. Introduction

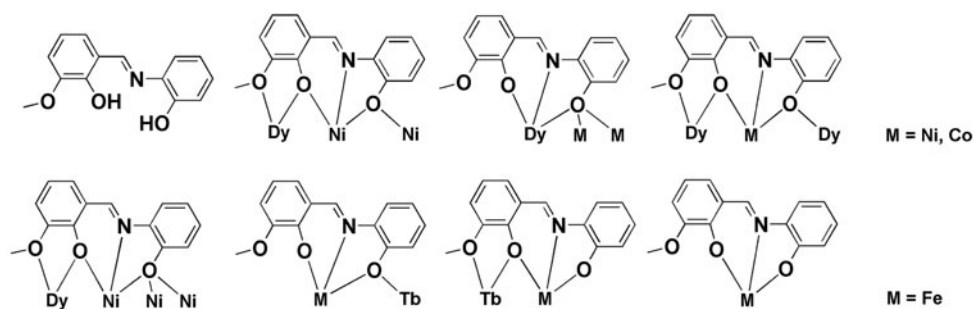
Anions occupy a preeminent place in crystal engineering for strong and directional interactions such as metal coordination, hydrogen bonding, halogen bonding, and anion- π (or weak σ) interactions. From a structural point of view, anions often affect crystal structures via templating and/or engaging in crystal assembly as building units or secondary building unit components [1]. It is common to find some anions directly coordinated [2]. Some noteworthy examples in coordination chemistry for crystals with various topologies and structural motifs include nitrate (NO₃⁻) [3], nitrite (NO₂⁻) [4], perchlorate (ClO₄⁻) [5], acetate (CH₃COO⁻) [6], triflate (CF₃SO₃⁻) [7], tetrafluoroborate (BF₄⁻) [5(d), 7(b), 8], thiocyanate (SCN⁻) [7(d), 9], sulfate (SO₄²⁻) [10], pivalic acid ((CH₃)₃CCOO⁻) [11], azide (N₃⁻) [12], and halide (X = F⁻, Cl⁻, Br⁻, I⁻) [5(a), 7(c), 13].

Carbonate (CO₃²⁻) has interest because the coordination mode of each oxygen is flexible with monodentate, bidentate, and tridentate, leading to various binding modes and yielding more and more carbonate-bridged compounds with different kinds of metal ions (scheme 1). These compounds possess nuclearities ranging from mono- [14] to deca- [15], dodeca- [12 (a), 16], trideca- [17], tetradeca- [18], octadeca- [19], icositetra- [13(a)], icosihexa- [20], and even dopentaconta-nuclear [21(a)]. There are 21 types of carbonate coordination modes established by literature (scheme 1). The two main methods employed to prepare carbonate-bridged complexes involve addition of carbonate salts or atmospheric carbon dioxide fixation.

Previous research covering carbonate-bridged compounds concentrated on transition metal ions such as Ni^{II} [12(a), 15], Co^{II} [15(i), 22], Cu^{II} [5(b), 23], Zn^{II} [15(h), 23, 24], Cd^{II} [15(d)], and light rare-earth ions such as La^{III} [15(h), 16(a), 17, 19], Ce^{III} [17], and Pr^{III} [15(e), (l), 17]. However, some work devoted to molecular magnetism contained heavy lanthanide ions (especially Dy^{III}) [15(b), (c), (h), and (i), 16(b)]. The hope has been to take advantage of their large magnetic moments and significant magnetic anisotropy to create single molecule magnets with highly effective relaxation energy barrier and improved properties. Surprisingly, only limited examples of carbonate-templated 3d-4f heterospin carriers



Scheme 1. The structurally characterized coordination modes of carbonate bridges.

Scheme 2. H_2L and its coordination modes.

[18(a), 21] have been reported through self-assembly of atmospheric carbon dioxide as the template agent [15(e), 18(a), 21].

Solvent also plays a crucial role in coordination chemistry inducing structural modification of crystals and the resultant magneto-structural correlations [25]. For example, recently, we demonstrated that two Dy-related cubanes [26] featuring $[Dy_4(\mu_3-OH)_4]$ core display distinct dynamic magnetic behavior through simply varying the reaction solvent. Recent work

indicates that ditopic 2-(2-hydroxy-3-methoxybenzylideneamino)phenol (H₂L) can yield several polynuclear and mixed 3d–4f metal clusters [27] (scheme 2). Our ongoing activities to synthesize new 3d–4f clusters with the 2-(2-hydroxy-3-methoxybenzylideneamino)phenol (H₂L) ligand expand the repertoire of this ligand for preparing 3d–4f heterometallic complexes. Herein, we describe the syntheses, structures, and magnetic investigations of four heterometallic dodecanuclear Ni–RE clusters, which feature tetra-capped hexahedron topology with four μ₅-bridged carbonates, [Ni^{II}₈RE^{III}₄(L)₈(CO₃)₆(H₂O)₁₄]·mCH₃OH·12H₂O [RE = Gd (**1**), *m* = 2; Dy (**2**), *m* = 0], and [Ni^{II}₈RE^{III}₄(L)₈(CO₃)₄(CH₃OH)₄(H₂O)₈]·(ClO₄)₄·8H₂O [RE = Dy (**3**), Y (**4**)], depending on the solvent used in the reaction systems.

2. Experimental

2.1. Materials

All reagents were purchased from commercial sources and used without purification. All RE(NO₃)₃·nH₂O were prepared from dissolving rare-earth oxides in concentrated nitric acid, respectively. The ligand 2-(2-hydroxy-3-methoxybenzylideneamino)phenol, abbreviated as H₂L, was prepared by condensation of 2-aminophenol and *o*-vanillin in a 1 : 1 M ratio in hot ethanol according to a modified procedure reported previously [28]. All reactions were carried out under aerobic conditions.

Caution: Perchlorate salts of metal complexes containing organic ligands are potentially explosive. Although no problems were encountered in the course of our synthesis, only small amounts of material should be prepared and handled with proper care.

2.2. Synthesis

2.2.1. [Ni₈Gd₄(L)₈(CO₃)₆(H₂O)₁₄]·2CH₃OH·12H₂O (1**).** To a stirred solution of H₂L (0.20 mM, 53 mg) in ethanol (25 mL), methanolic solution of triethylamine (1.60 mL, 0.80 mM) was added. The resulting deep red solution was stirred at room temperature for 1 h before solid Gd(NO₃)₃·6H₂O (0.20 mM, 93 mg) was added. The resulting yellow solution was stirred at room temperature for 3 h. Solid Ni(ClO₄)₂·6H₂O (0.40 mM, 150 mg) was added and further stirred for 3 h. The brown mixture was filtered and the filtrate was left undisturbed to allow slow evaporation of the solution. Deep brown block single crystals, suitable for X-ray diffraction analysis, were obtained after 2 weeks. These crystals were collected by filtration, washed with cold ethanol, and dried in air. Yield: 50 mg (25%, based on the metals). Elemental analysis (%) calcd for C₁₂₀H₁₄₈N₈O₇₀Ni₈Gd₄: C, 36.75; H, 3.80; N, 2.86. Found: C, 36.24; H, 4.05; N, 3.05. IR (KBr, cm⁻¹): 3360(m), 3061(w), 1618(s), 1587(m), 1553(m), 1512(m), 1481(s), 1461(s), 1411(s), 1386(s), 1305(s), 1291(s), 1257(m), 1225(m), 1183(m), 1153(w), 1111(w), 1095(w), 1077(m), 1040(w), 968(s), 877(w), 857(w), 824(s), 781(w), 734(m), 640(w), 626(w), 576(w), 556(w), 516(m), 442(w).

2.2.2. [Ni₈Dy₄(L)₈(CO₃)₆(H₂O)₁₄]·12H₂O (2**).** This complex was obtained as deep brown block crystals according to the procedure for **1** using Dy(NO₃)₃·6H₂O (0.20 mM, 98 mg) in place of Gd(NO₃)₃·6H₂O. Yield: 44 mg (22%, based on the metals). Elemental analysis (%) calcd for C₁₁₈H₁₄₀N₈O₆₈Ni₈Dy₄: C, 36.54; H, 3.64; N, 2.89. Found: C, 36.20; H, 3.87; N, 3.02. IR (KBr, cm⁻¹): 3199(w), 3060(w), 2948(w), 1618(s), 1587(m), 1553(m), 1519(m),

1481(s), 1462(s), 1407(s), 1387(s), 1306(s), 1290(s), 1254(m), 1225(m), 1183(m), 1153(m), 1095(w), 1075(m), 966(s), 876(w), 856(w), 823(s), 781(w), 734(m), 641(w), 624(w), 576(w), 557(w), 517(m), 444(w).

2.2.3. $[\text{Ni}_8\text{Dy}_4(\text{L})_8(\text{CO}_3)_4(\text{CH}_3\text{OH})_4(\text{H}_2\text{O})_8] \cdot (\text{ClO}_4)_4 \cdot 8\text{H}_2\text{O}$ (3). To a stirred solution of H_2L (0.20 mM, 52 mg) in methanol (35 mL) was added a methanolic solution of triethylamine (1.60 mL, 0.80 mM). The resulting deep red solution was stirred at room temperature for 1 h before solid $\text{Dy}(\text{NO}_3)_3 \cdot 6\text{H}_2\text{O}$ (0.20 mM, 96 mg) was added. The resulting yellow solution was stirred at room temperature for 3 h. Solid $\text{Ni}(\text{ClO}_4)_2 \cdot 6\text{H}_2\text{O}$ (0.40 mM, 148 mg) was added and further stirred for 3 h. The brown mixture was filtered and the filtrate was left undisturbed to allow slow evaporation of the solution. Deep brown block single crystals, suitable for X-ray diffraction analysis, were obtained after 12 days. These crystals were collected by filtration, washed with cold ethanol, and dried in air. Yield: 55 mg (27%, based on the metals). Elemental analysis (%) calcd for $\text{C}_{120}\text{H}_{136}\text{N}_8\text{O}_{72}\text{Cl}_4\text{Ni}_8\text{Dy}_4$: C, 35.12; H, 3.34; N, 2.73. Found: C, 34.91; H, 3.74; N, 2.65. IR (KBr, cm^{-1}): 3351(m), 1618(s), 1587(m), 1553(m), 1517(m), 1481(s), 1462(s), 1408(s), 1387(s), 1307(s), 1291(s), 1255(m), 1226(m), 1183(m), 1152(w), 1094(w), 966(s), 877(w), 856(w), 823(s), 781(w), 735(m), 639(w), 626(w), 576(w), 558(w), 517(m), 444(w).

2.2.4. $[\text{Ni}_8\text{Y}_4(\text{L})_8(\text{CO}_3)_4(\text{CH}_3\text{OH})_4(\text{H}_2\text{O})_8] \cdot (\text{ClO}_4)_4 \cdot 8\text{H}_2\text{O}$ (4). This compound was obtained as deep brown block crystals according to the procedure for **3** using $\text{Y}(\text{NO}_3)_3 \cdot 5\text{H}_2\text{O}$ (0.20 mM, 75 mg) in place of $\text{Dy}(\text{NO}_3)_3 \cdot 6\text{H}_2\text{O}$. Yield: 50 mg (26%, based on the metals). Elemental analysis (%) calcd for $\text{C}_{120}\text{H}_{136}\text{N}_8\text{O}_{72}\text{Cl}_4\text{Ni}_8\text{Y}_4$: C, 37.83; H, 3.60; N, 2.94. Found: C, 37.56; H, 3.89; N, 2.97. IR (KBr, cm^{-1}): 3350(m), 1617(s), 1587(m), 1553(m), 1522(m), 1481(s), 1463(s), 1409(s), 1386(s), 1308(s), 1290(s), 1255(m), 1226(m), 1183(m), 1152(w), 1094(w), 966(s), 876(w), 857(w), 823(s), 782(w), 736(m), 640(w), 626(w), 576(w), 559(w), 518(m), 445(w).

2.3. Methods

The C, H, and N elemental analyses were performed on a VarioEL element analyzer. Infrared (IR) measurements were recorded on a VERTEX 70 Fourier transform infrared spectrophotometer using the reflectance technique ($4000\text{--}300\text{ cm}^{-1}$); the samples were prepared as KBr disks. Powder X-ray diffraction (PXRD) analyses were performed on a Bruker D8-Advance diffractometer with $\text{Cu-K}\alpha$ (1.54059 \AA) radiation at a scan speed of 10°min^{-1} . Magnetic measurements were performed from 2 to 300 K using a Quantum Design MPMS XL-7 SQUID magnetometer equipped with a 7 T magnet. Diamagnetic corrections for all the compounds were estimated using Pascal's constants, and magnetic data were corrected for diamagnetic contribution of the sample holder. For magnetization experiments, the temperature was set from 1.9 to 5 K and the field was varied from 0 to 7 T. Samples were restrained in eicosane to prevent torquing. Alternating current susceptibility measurements were taken of powdered **1–4** to determine the in-phase and out-of-phase components of the magnetic susceptibility. The data were collected by decreasing temperature from 30 to 1.9 K, with no applied external dc field and a drive frequency of 3 Oe, with frequencies between 1 and 1200 Hz.

Table 1. Crystallographic data and structure refinement summaries for 1–4.

Compound	1	2	3	4
Empirical formula	C ₁₂₀ H ₁₄₈ Ni ₈ O ₇₀ Ni ₈ Gd ₄	C ₁₁₈ H ₁₄₀ Ni ₈ O ₆₈ Ni ₈ Dy ₄	C ₁₂₀ H ₁₃₆ Ni ₈ O ₇₂ Cl ₄ Ni ₈ Dy ₄	C ₁₂₀ H ₁₃₆ Ni ₈ O ₇₂ Cl ₄ Ni ₈ Y ₄
Formula mass	3921.14	3878.06	4103.85	3809.49
Crystal system	Tetragonal	Tetragonal	Tetragonal	Tetragonal
<i>a</i> (Å)	16.7919(7)	16.7034(5)	21.0722(8)	21.0018(10)
<i>b</i> (Å)	16.7919(7)	16.7034(5)	21.0722(8)	21.0018(10)
<i>c</i> (Å)	26.341(2)	26.1793(15)	17.6647(13)	17.6007(17)
α (°)	90.00	90.00	90.00	90.00
β (°)	90.00	90.00	90.00	90.00
γ (°)	90.00	90.00	90.00	90.00
<i>U</i> (Å ³)	7427.4(7)	7304.1(5)	7843.8(7)	7763.2(9)
<i>T</i> (K)	185(2)	185(2)	185(2)	185(2)
Space group	<i>P</i> 42/ <i>c</i>	<i>P</i> 42/ <i>c</i>	<i>P</i> 42/ <i>n</i>	<i>P</i> 42/ <i>n</i>
<i>Z</i>	2	2	2	2
Data measured	36,835	36,502	39,099	41,680
Unique data	6545	6504	6980	7672
<i>R</i> _{int}	0.0629	0.0487	0.0592	0.1076
<i>R</i> ₁ [<i>I</i> > 2 σ (<i>I</i>)]	0.0455	0.0433	0.0608	0.0860
w <i>R</i> (<i>F</i> ²) [<i>I</i> > 2 σ (<i>I</i>)]	0.1293	0.1316	0.1750	0.2285
<i>R</i> ₁ (all data)	0.0511	0.0486	0.0871	0.1629
w <i>R</i> (<i>F</i> ²) (all data)	0.1328	0.1377	0.1952	0.2692
<i>S</i> (all data)	1.096	1.167	1.145	1.139

2.4. X-ray crystal structure determination

Single-crystal X-ray diffraction data were collected on a Bruker Apex II CCD diffractometer with graphite-monochromated Mo K α radiation ($\lambda = 0.71073$ Å). All collections were performed at $T = 185(2)$ K. Data processing was accomplished with the SAINT processing program. Crystal structures were solved by direct methods (SHELXTL97) [29] with subsequent refinement with the SHELXTL97 software package. The locations of the heaviest atoms (Ni and RE) were easily determined, and O, N, and C were subsequently determined from the difference Fourier maps. The non-hydrogen atoms were refined anisotropically. Hydrogens were introduced in calculated positions and refined with fixed geometry with respect to their carrier atoms.

Crystallographic data and refinement details for **1–4** are summarized in table 1. Selected bond lengths and angles of **1–4** are given in table S1 (see online supplemental material at <http://dx.doi.org/10.1080/00958972.2015.1004326>) in the Supporting Information.

3. Results and discussion

3.1. Structure description

The reaction of $\text{RE}(\text{NO}_3)_3 \cdot 6\text{H}_2\text{O}$ (RE = Gd, Dy), $\text{Ni}(\text{ClO}_4)_2 \cdot 6\text{H}_2\text{O}$, H₂L, and NEt_3 in a 1 : 2 : 1 : 4 stoichiometry in a mixture of methanol and ethanol leads to two isostructural dodecanuclear heterobimetallic clusters, $[\text{Ni}^{\text{II}}_8\text{RE}^{\text{III}}_4(\text{L})_8(\text{CO}_3)_6(\text{H}_2\text{O})_{14}] \cdot m\text{CH}_3\text{OH} \cdot 12\text{H}_2\text{O}$ [RE = Gd (**1**), $m = 2$; Dy (**2**), $m = 0$]. The structure of **2** is described here as a representative (figure 1).

Complex **2** crystallizes in a tetragonal space group. There are only three metal ions (Ni1, Ni2, and Dy1) in the asymmetric unit. Both Ni1 and Ni2 are six-coordinate with distorted octahedral geometries. Ni1 has a NO_5 set of donors arising from two ligands and two carbonate anions. The coordination sites of Ni2 are occupied by NO_3 donors of two ligands, one oxygen from carbonate and a disordered terminal ligand comprising of either carbonate or water with equal occupancy. Carbonate and water are coordinated to Ni2 with a disorder over two possible sites, whose site-occupancy factor is 0.5. Dy1 is nine-coordinate with a DyO_9 coordination sphere originating from two ligands and two carbonates in addition to three terminal coordinated waters. The coordination geometry of Dy1 adopts a distorted mono-capped square antiprism, which is composed of two planes; O4a, O7, O13, and O15 define the upper plane while O1, O2, O5a, and O9a occupy the lower plane with O14 at the mono-capped position. Ni1 is triply bridged to Ni2 through one carbonate and two phenol oxygens from the 2-aminophenol of two ligands. In addition, Ni1 is triply linked to Dy1 through two carbonates and one phenol oxygen from the *o*-vanillin of the ligand. Ni2 is connected to Dy1 through the carbonate bridge. The Ni–O–Ni and Ni–O–Dy angles range from 88.0(2) to 89.4(2) and 99.8(2) to 107.5(2), respectively.

Four μ_5 -carbonate bridges hold four Ni_2Dy asymmetric units together forming a dodecanuclear cluster, which can be viewed as an irregular tetra-capped hexahedron topology (figure 1, bottom). Dy1, Ni1, and their symmetry equivalents alternately occupy the apical positions of the hexahedron, while Ni2 and its symmetry equivalents locate at the cap sites. The Ni \cdots Ni and Ni \cdots Dy as well as Dy \cdots Dy distances are 2.9136–5.9610, 3.3804–5.3437, and 6.8493–7.9356 Å.

Reactions of H₂L with $\text{RE}(\text{NO}_3)_3 \cdot n\text{H}_2\text{O}$ (RE = Dy, Y), $\text{Ni}(\text{ClO}_4)_2 \cdot 6\text{H}_2\text{O}$, and NEt_3 in a 1 : 1 : 2 : 4 M ratio in methanol yield two isostructural dodecanuclear heterobimetallic

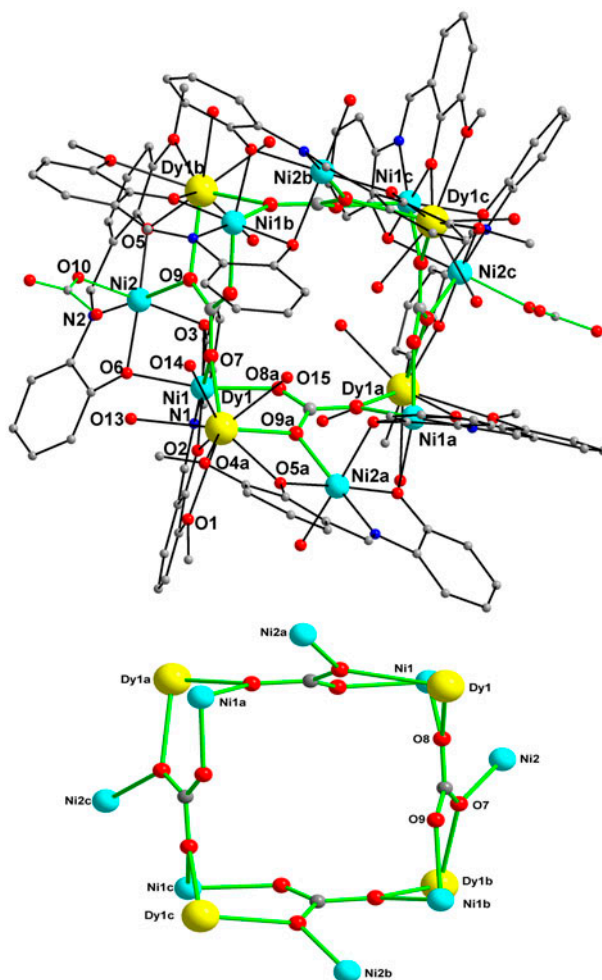


Figure 1. (top) Molecular structure of **2**. Hydrogens and solvent are omitted for clarity. Symmetry codes: (a) = $x, -y, 2 - z$; (b) = $-x, y, 2 - z$; (c) = $-x, -y, z$. Color scheme: Dy^{III}, yellow; Ni^{II}, turquoise; O, red; N, blue; C, gray. The bright green bold lines highlight carbonate anions (bottom). The tetra-capped hexahedron topology bridged by four μ_5 -bridged carbonate anions (see <http://dx.doi.org/10.1080/00958972.2015.1004326> for color version).

clusters, $[\text{Ni}^{\text{II}}_8\text{RE}^{\text{III}}_4(\text{L})_8(\text{CO}_3)_4(\text{CH}_3\text{OH})_4(\text{H}_2\text{O})_8] \cdot (\text{ClO}_4)_4 \cdot 8\text{H}_2\text{O}$ [RE = Dy (**3**), Y (**4**)]. The tiny difference in the synthetic procedure for **1–4** only lies in the solvent used in the course of the reaction.

Compounds **1** and **2** are acquired in a mixture of ethanol and methanol, whereas **3** and **4** crystallize from methanol. A comparison of the molecule structures of **1** and **2** with those of **3** and **4** shows them to be very similar. For simplicity, we provide crystal structure of **3** shown in figure 2. Solvent merely imposes subtle differences on the crystal core structure with three dissimilarities extracted from their core structures: first, carbonate or water with equal occupancy coordinates to Ni2 with a monodentate mode in **1** and **2** while it changes to methanol in **3** and **4**; second, the coordination number of the rare-earth ions in **1** and **2** is nine *versus* eight in **3** and **4** as a result of the number of coordinated waters reducing from

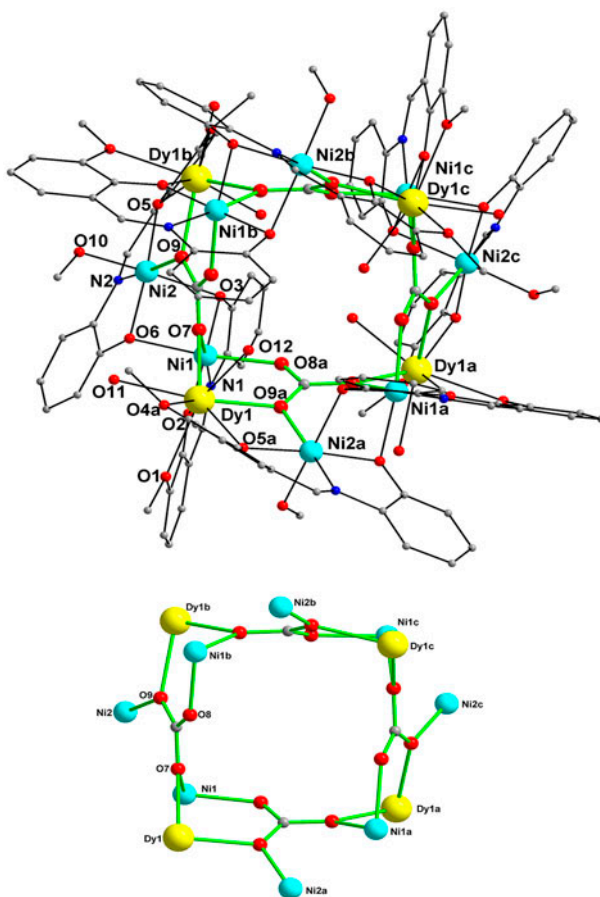


Figure 2. (top) molecular structure of **3**. Hydrogens and solvent are omitted for clarity. Symmetry codes: (a) $x, \frac{1}{2} - y, \frac{3}{2} - z$; (b) $\frac{1}{2} - x, y, \frac{3}{2} - z$; (c) $\frac{1}{2} - x, \frac{1}{2} - y, z$. Color scheme: Dy^{III}, yellow; Ni^{II}, turquoise; O, red; N, blue; C, gray. The bright green bold lines highlight carbonate anions (bottom). The tetra-capped hexahedron topology bridged by four μ_5 -carbonate bridges (see <http://dx.doi.org/10.1080/00958972.2015.1004326> for color version).

three to two; finally, the core structure of **1** and **2** is neutral in comparison with that of **3** and **4** as a tetravalent cation, in which four dissociated perchlorates are counteranions. Dy1 in **3** is eight-coordinate in a distorted square antiprismatic environment of eight oxygens from two ligands and two carbonates as well as two terminal coordinated waters. One square face consists of O1, O2, O5a, and O9a while the other corresponds to O4a, O7, O11, and O12.

In the present case, the carbonate is explained by fixation of atmospheric CO₂ from the air in basic media, and the identification of CO₃²⁻ ion was determined by charge balance and careful consideration of the X-ray diffraction data. Furthermore, strong carbonate-related infrared (IR) vibration bands are present at 1461–1463 cm⁻¹ in all the complexes [15h]. Additionally, the standard distance of NO₃⁻ is 1.21 Å and the standard distance of CO₃²⁻ is 1.28 Å. The distances of anions for the synthesized four complexes are as follows: **1**: $d = 1.306, 1.276$ and 1.272 Å; **2**: $d = 1.269, 1.281,$ and 1.291 Å; **3**: $d = 1.289, 1.252,$

and 1.309 Å; **4**: $d = 1.265, 1.285, \text{ and } 1.286 \text{ \AA}$. Obviously, the practical distances of anions of all the complexes agree with the theoretical distances of CO_3^{2-} anion.

The phase purities of **1–4** were confirmed by PXRD measurements conducted at room temperature (figure S1). All the PXRD patterns performed on the as-synthesized samples were in agreement with the PXRD patterns simulated from the respective single-crystal X-ray diffraction data, confirming the phase purity of the synthesized samples.

It should be stressed here that the structures of **1–4** are markedly different to the previous $\text{Ni}^{\text{II}}_8\text{Gd}^{\text{III}}_4$ cluster reported by Hooper *et al.* [30], in which the core structure comprises a square (or wheel) of four corner-sharing $[\text{Ni}^{\text{II}}_2\text{Gd}^{\text{III}}_2\text{O}_4]^{6+}$ cubanes. Additionally, our complexes join only a handful of high-nuclearity $\text{Ni}^{\text{II}}\text{--RE}^{\text{III}}$ families such as $\text{Ni}^{\text{II}}_6\text{RE}^{\text{III}}_6$ (RE = Gd, Dy, Y), $\text{Ni}^{\text{II}}_2\text{RE}^{\text{III}}_{12}$ (RE = Tb, Dy), $\text{Ni}^{\text{II}}_8\text{Dy}^{\text{III}}_8$, $\text{Ni}^{\text{II}}_{12}\text{Gd}^{\text{III}}_{36}$, $\text{Ni}^{\text{II}}_{10}\text{RE}^{\text{III}}_{42}$ (RE = Gd, Dy), $\text{Ni}^{\text{II}}_{76}\text{La}^{\text{III}}_{60}$ clusters [18(a), 21(a), 31] with a wide variety of structure motifs.

3.2. Magnetic properties

Static magnetic studies were measured on **1–4**, and the temperature dependence of their magnetic susceptibilities is shown as $\chi_M T$ versus T in figure 3, χ_M being the molar magnetic susceptibility of the dodecanuclear species.

Complex **4** with four diamagnetic Y^{III} ions will be described first for it represents the simplest example. The $\chi_M T$ product for **4** at room temperature is $9.81 \text{ cm}^3 \text{ K M}^{-1}$, which is very close to the theoretical value ($9.68 \text{ cm}^3 \text{ K M}^{-1}$) corresponding to eight uncoupled Ni^{II} ($S = 1, g = 2.2, \text{ and } C = 1.21 \text{ cm}^3 \text{ K M}^{-1}$) ions. On decreasing the temperature, the $\chi_M T$ product slowly increases to $10.26 \text{ cm}^3 \text{ K M}^{-1}$ at 45 K. Below 45 K, the $\chi_M T$ product steeply decreases and reaches a value of $1.24 \text{ cm}^3 \text{ K M}^{-1}$ at 2 K. The increase of $\chi_M T$ with lowering the temperature from 45 to 300 K indicates ferromagnetic interactions among the intramolecular Ni^{II} ions, the sharp decrease of $\chi_M T$ at lower temperature being due to intermolecular antiferromagnetic interactions and/or due to zero-field splitting factor. Initially, we attempted to fit the magnetic susceptibility curve with eight Ni^{II} paramagnetic centers,

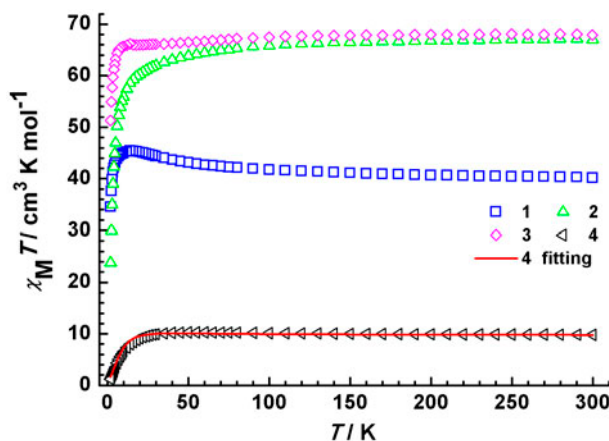


Figure 3. Plots of $\chi_M T$ vs. T for **1–4** from 2 to 300 K under an applied dc field of 1000 Oe. The red solid lines indicate the fitting using the theoretical model (see text) (see <http://dx.doi.org/10.1080/00958972.2015.1004326> for color version).

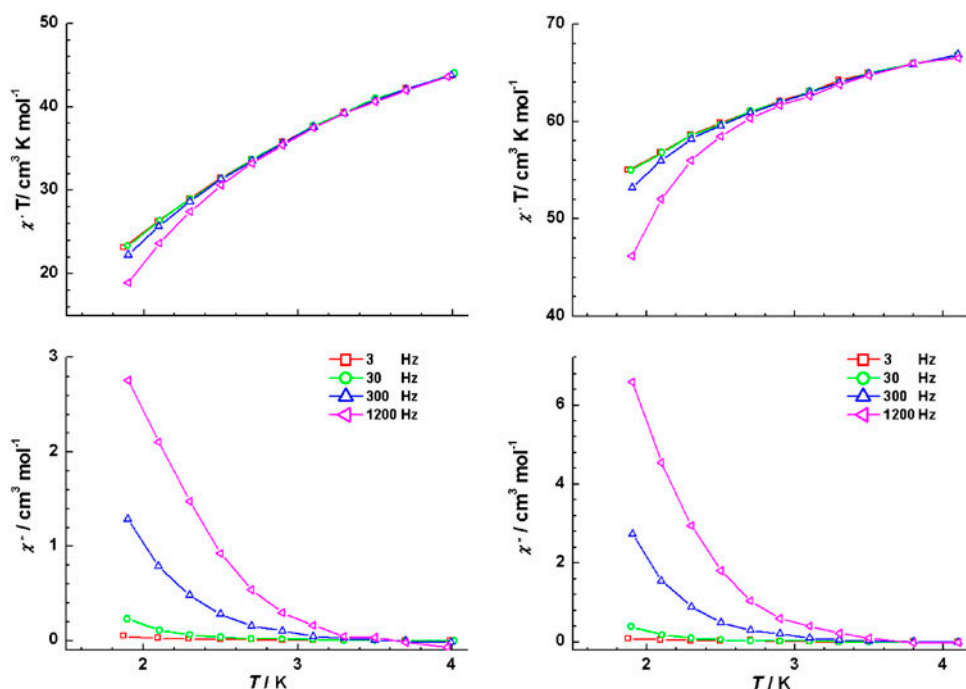


Figure 4. Temperature dependence of AC susceptibilities for **2** (left) and **3** (right) of in-phase (as $\chi'T$) (top) and out-of-phase (bottom) at the indicated frequencies under zero static field.

in order to extract the exchange interactions among Ni^{II} ions and single ion zero-field splitting parameter D . However, it failed due to the large size of the Hamiltonian matrix. Taking into account the crystal structure, where **4** crystallizes in a tetragonal space group and the asymmetric unit contains two Ni^{II} ions (Ni1 and Ni2), the following Hamiltonian has been chosen to roughly reproduce the experimental magnetic susceptibility data, where S_{Ni1} and S_{Ni2} are spin operators on ions of Ni1 and Ni2 , respectively, J_1 denotes the interaction between Ni1 and Ni2 , and D is the axial zero-field splitting parameter. The experimental data were successfully simulated using the *MAGPACK* [32] package of programs. The best set of parameters is $J_1 = 1.8 \text{ cm}^{-1}$,

$$\hat{H} = -2J_1(\hat{S}_{\text{Ni1}} \cdot \hat{S}_{\text{Ni2}}) + D \sum_{i=1}^2 (\hat{S}_{iz}^2 - \hat{S}_i(\hat{S}_i + 1)/3)$$

$|D| = 22 \text{ cm}^{-1}$ and $g = 2.20$. It should be noted that we could not determine the sign of D from magnetic susceptibility data derived from measurements on polycrystalline samples [33]. The D value obtained with the fit is large for standard Ni^{II} ions, which may be due to other antiferromagnetic $\text{Ni} \cdots \text{Ni}$ pathways [34]. The field dependence of magnetization was recorded at 2 K for **4** (figure S2 in Supporting Information), which illustrates $M(H)$ rising with applied field and reaching $9.6 \mu_{\text{B}}$ at 7 T with no sign of saturation. The magnetization data cannot be satisfactorily simulated with the same set of parameters obtained from the fit of $\chi_{\text{M}}T$ data.

The $\chi_M T$ product of **1** at room temperature is $40.15 \text{ cm}^3 \text{ K M}^{-1}$, which is in accord with the expected value of $41.18 \text{ cm}^3 \text{ K M}^{-1}$ for non interacting eight Ni^{II} ($S = 1$, $g = 2.2$, and $C = 1.21 \text{ cm}^3 \text{ K M}^{-1}$) and four Gd^{III} (${}^8S_{7/2}$, $S = 7/2$, $L = 0$, $J = 7/2$, $g = 2$, and $C = 7.875 \text{ cm}^3 \text{ K M}^{-1}$) ions. On lowering the temperature, $\chi_M T$ increases gradually to reach a maximum value of $45.39 \text{ cm}^3 \text{ K M}^{-1}$ at 14 K followed by a pronounced drop to a value of $35.52 \text{ cm}^3 \text{ K M}^{-1}$ at 2 K. The increase of $\chi_M T$ with lowering the temperature indicates intramolecular ferromagnetic interactions between the metal centers. The rapid drop of $\chi_M T$ at low temperature may be attributed to either zero-field splitting or intermolecular antiferromagnetic interactions. It is not possible to evaluate magnetic exchange interaction parameters in **1** by fitting the experimental magnetic data taking into account the fact that the nuclearity numbers of them are 12 (eight Ni^{II} and four Gd^{III} ions), and bridged modes between the spin carriers are complicated. The field dependence of the magnetization for **1** at 2 K shows an initial sharp increase for fields up to 2 T, reaching $31.48 \mu_B$ followed by a slower quasi-linear increase up to 7 T, at which it is $37.36 \mu_B$ (figure S3 in the Supporting Information).

At room temperature, the $\chi_M T$ values are 66.99 and $67.91 \text{ cm}^3 \text{ K M}^{-1}$ for **2** and **3**, respectively, being close to the expected values of $66.36 \text{ cm}^3 \text{ K M}^{-1}$ for eight uncoupled Ni^{II} ($S = 1$, $g = 2.2$, and $C = 1.21 \text{ cm}^3 \text{ K M}^{-1}$) and four Dy^{III} (${}^6H_{15/2}$, $S = 5/2$, $L = 5$, $J = 7/2$, $g = 4/3$, and $C = 14.17 \text{ cm}^3 \text{ K M}^{-1}$) ions. For **2** and **3**, the $\chi_M T$ products decrease slowly above 110 and 65 K and then rapidly drop at lower temperatures reaching values of 23.81 and $51.30 \text{ cm}^3 \text{ K M}^{-1}$ at 2 K. The gradual decrease of $\chi_M T$ above 110 and 65 K for **2** and **3** is ascribed mainly to the thermal depopulation of the Dy^{III} excited states, while the sharp drop of $\chi_M T$ below 110 and 65 K for **2** and **3** suggests antiferromagnetic exchange interactions between metal centers. This behavior in $\chi_M T$ curves suggests that the ligand field and/or magnetic interactions between the Dy^{III} ions are different in **2** and **3**. At low temperatures, the magnetization data of **2** and **3** were obtained (figure S4 in Supporting Information). The non-superposition of the reduced magnetization plots indicates the presence of significant magnetic anisotropy and/or low-lying excited states. The magnetization value of **2** at 1.9 K and 7 T is $31.65 \mu_B$ and lower than that of **3**, which is $36.71 \mu_B$.

The presence of magnetic anisotropy was probed by AC susceptibility measurements for **2** and **3** at varied frequencies. As shown in the top panels of figure 4, the $\chi' T$ values decrease upon lowering the temperature and the $\chi' T$ values for all the frequencies below 1200 Hz converge at 2.7 K for **2** and 3.4 K for **3**. Moreover, the $\chi' T$ values are virtually identical with the χT values obtained from static dc field under 1000 Oe. The extrapolation of $\chi' T$ to the intersections of the Y axes suggests **2** and **3** have different spin ground states. Frequency-dependent out-of-phase (χ'') signals are observed below 3.3 K for **2** and 3.5 K for **3**, indicating the presence of slow magnetic relaxation. However, no peaks were observed, which is mainly due to the fast quantum tunneling of the magnetization.

Single ion magnetic anisotropy is strongly sensitive to minor structural details. The distinct slow magnetic relaxation behavior shown in **2** and **3** is probably associated with slight changes in the crystal structures, primarily manifested by the coordination environment modifications of Dy^{III} ions. The coordination number of Dy^{III} in **2** is nine in mono-capped square antiprism geometry, while it changes to square antiprism polyhedron with eight coordination in **3**. Such coordination environment changes between **2** and **3** are from coordinated water. Three water molecules bound to Dy^{III} ions in **2** and two water molecules coordinated to Dy^{III} in **3**. The average Dy–O_{water} distances (2.441 Å) of **2** are longer than the average Dy–O_{water} distances (2.387 Å) of **3** (table S1). The additional water molecule and minute variations in bond distances around Dy^{III} centers result in differences in the

local anisotropy of Dy^{III} ions [35]. Obviously, different coordination environments lead to different symmetry and strength of ligand field of Dy^{III} ions, which may also affect the nature or direction of the easy axes [36].

Dynamic magnetic behavior in 4f-SMMs can be tuned by axial ligand or anion [37]. Single ion magnetic anisotropy is probably the most important factor, which moderates the magnetic relaxation. The exchange interactions between Dy^{III} ions and the spatial arrangement of Dy^{III} ions that modulate the magnetic relaxation cannot be ruled out. A complete and detailed elucidation of the magnetic relaxation distinction in **2** and **3** is a challenging task. Our work demonstrates that the coordination geometry around Dy^{III} ions was transformed between distorted mono-capped square antiprism in **2** and square antiprism in **3** by coordination of one additional terminal water, which led to changes in the strength and direction of the magnetic anisotropy axis [38].

4. Conclusion

Two synthetic procedures through atmospheric CO₂ fixation reactions gave four heterometallic dodecanuclear clusters with molecular formulas [Ni^{II}₈RE^{III}₄(L)₈(CO₃)₆(H₂O)₁₄]·mCH₃OH·12H₂O [RE = Gd (**1**), *m* = 2; Dy (**2**), *m* = 0] and [Ni^{II}₈RE^{III}₄(L)₈(CO₃)₄(CH₃OH)₄(H₂O)₈]·(ClO₄)₄·8H₂O [RE = Dy (**3**), Y (**4**)]. The tiny difference in the synthetic procedure for **1–4** lies in the solvent used in the reaction. Ethanol and methanol mixed solvent leads to **1** and **2**, whereas methanol results in **3** and **4**. The overall structure of these clusters features a “tetra-capped hexahedron” topology bridged by four μ₅-carbonate bridges. Analysis of static susceptibility data shows the presence of dominant ferromagnetic interactions between the metal centers in **1** and **4**. Comparisons of the static and dynamic magnetic behavior of **2** and **3** suggest that modifications in the crystal structure such as different coordination environment around Dy^{III} ions may affect the nature or directions of the magnetic anisotropic axes, caused by coordination perturbation [39]. This synthetic approach encourages us to prepare heterometallic clusters while retaining essentially the same core structure by changing solvent or anion.

Supplementary material

CCDC 902449, 902450, 902452 and 902453 for **1–4** contain the supplementary crystallographic data. These data can be obtained free of charge via <http://www.ccdc.cam.ac.uk/contents/retrieving.html> or from the Cambridge Crystallographic Data Center, 12 Union Road, Cambridge CB2 1EZ, UK (Fax: +44 (0)-1223-336033; E-mail: deposit@ccdc.cam.ac.uk).

Funding

This work was supported by Natural Science Foundation of China [grant number 21073142]; Education Committee of Shaanxi Province [grant number 11JK0812]; the start-up foundation of Northwest University [grant number PR13094]; the school fund of Northwest University [grant number NF14023].

Supplemental data

Selected bond lengths and angles for 1–4 (table S1), additional powder X-ray diffraction data and magnetic data for 1–4 (figures S1–S4) are shown in supporting information.

References

- [1] R. Custelcean. *Chem. Soc. Rev.*, **39**, 3675 (2010).
- [2] R. Díaz-Torres, S. Alvarez. *Dalton Trans.*, **40**, 10742 (2011).
- [3] (a) X. Gu, D. Xue. *Inorg. Chem.*, **46**, 3212 (2007); (b) B. Cristóvão, J. Klak, B. Miroslaw. *J. Coord. Chem.*, **67**, 2728 (2014).
- [4] (a) A.O. Borodin, G.A. Kostin, P.E. Plusnin, E.Y. Filatov, A.S. Bogomyakov, N.V. Kuratieva. *Eur. J. Inorg. Chem.*, 2298 (2012); (b) A. Pons-Balagué, N. Ioanidis, W. Wernsdorfer, A. Yamaguchi, E.C. Sañudo. *Dalton Trans.*, **40**, 11765 (2011).
- [5] (a) C.S. Campos-Fernández, B.L. Schottel, H.T. Chifotides, J.K. Bera, J. Bacsá, J.M. Koomen, D.H. Russell, K.R. Dunbar. *J. Am. Chem. Soc.*, **127**, 12909 (2005); (b) A. Escuer, F.A. Mautner, E. Peñalba, R. Vicente. *Inorg. Chem.*, **37**, 4190 (1998); (c) S. Ferrer, F. Lloret, E. Pardo, J.M. Clemente-Juan, M. Liu-González, S. García-Granda. *Inorg. Chem.*, **51**, 985 (2012); (d) W.A. Gobeze, V.A. Milway, B. Moubaraki, K.S. Murray, S. Brooker. *Dalton Trans.*, **41**, 9708 (2012).
- [6] (a) M. Manoli, R. Inglis, M.J. Manos, V. Nastopoulos, W. Wernsdorfer, E.K. Brechin, A.J. Tasiopoulos. *Angew. Chem. Int. Ed.*, **50**, 4441 (2011); (b) L. Saghatforoush, E. Sahin, S. Babaei, A. Bakhtiari, A. Nasimian, Ö. Çelik, Z. Zabihollahi. *J. Coord. Chem.*, **67**, 1463 (2014).
- [7] (a) L. Aboshyan-Sorgho, C. Besnard, P. Pattison, K.R. Kittilstved, A. Aebischer, J.G. Bünzli, A. Hauser, C. Piguet. *Angew. Chem. Int. Ed.*, **50**, 4108 (2011); (b) M.U. Anwar, A.S. Elliott, L.K. Thompson, L.N. Dawe. *Dalton Trans.*, **40**, 4623 (2011); (c) M.U. Anwar, K.V. Shuvaev, L.N. Dawe, L.K. Thompson. *Inorg. Chem.*, **50**, 12141 (2011); (d) E. Colacio, J.E. Perea-Buceta, A.J. Mota, E.K. Brechin, A. Hänninen, P. Seppälä, R. Sillanpää. *Chem. Commun.*, **48**, 805 (2012).
- [8] L. Botana, J. Ruiz, J.M. Seco, A.J. Mota, A. Rodríguez-Diéguez, R. Sillanpää, E. Colacio. *Dalton Trans.*, **40**, 12462 (2011).
- [9] (a) S. Biswas, S. Naiya, C.J. Gómez-García, A. Ghosh. *Dalton Trans.*, **41**, 462 (2012); (b) J.M. Clemente-Juan, C. Mackiewicz, M. Verelst, F. Dahan, A. Bousseksou, Y. Sanakis, J.-P. Tuchagues. *Inorg. Chem.*, **41**, 1478 (2012).
- [10] C.G. Efthymiou, A.A. Kitos, C.P. Raptopoulou, S.P. Perlepes, A. Escuer, C. Papatriantafyllopoulou. *Polyhedron*, **28**, 3177 (2009).
- [11] (a) S.K. Langley, R.A. Stott, N.F. Chilton, B. Moubaraki, K.S. Murray. *Chem. Commun.*, **47**, 6281 (2011); (b) G. Abbas, Y. Lan, G. Kostakis, C.E. Anson, A.K. Powell. *Inorg. Chim. Acta*, **361**, 3494 (2008); (c) A.M. Ako, V. Mereacre R. Clérac, I.J. Hewitt, Y. Lan, G. Buth, C.E. Anson, A.K. Powell. *Inorg. Chem.*, **48**, 6713 (2009).
- [12] (a) A.K. Ghosh, M. Pait, M. Shatruck V. Bertolasi, D. Ray. *Dalton Trans.*, **43**, 1970 (2014); (b) J. Rinck, G. Novitchi, W. Van den Heuvel, L. Ungur, Y. Lan, W. Wernsdorfer, C.E. Anson, L.F. Chibotaru, A.K. Powell. *Angew. Chem. Int. Ed.*, **49**, 7583 (2010); (c) D. Schray, G. Abbas, Y. Lan, V. Mereacre, A. Sundt, J. Dreiser, O. Waldmann, G.E. Kostakis, C.E. Anson, A.K. Powell. *Angew. Chem. Int. Ed.*, **49**, 5185 (2010).
- [13] (a) K.-C. Xiong, F.-L. Jiang, Y.-L. Gai, D.-Q. Yuan, D. Han, J. Ma, S.-Q. Zhang, M.-C. Hong. *Chem. Eur. J.*, **18**, 5536 (2012); (b) A. McRobbie, A.R. Sarvar, S. Yeninas, H. Nowell, M.L. Baker, D. Allan, M. Luban, C.A. Muryn, R.G. Pritchard, R. Prozorov, G.A. Timco, F. Tuna, G.F.S. Whitehead, R.E.P. Winpenny. *Chem. Commun.*, **47**, 6251 (2011); (c) G. Aromi, M.J. Knapp, J.-P. Claude, J.C. Huffman, D.N. Hendrickson, G. Christou. *J. Am. Chem. Soc.*, **121**, 5489 (1999); (d) L.J. Batchelor, M. Sangalli, R. Guillot, N. Guihéry, R. Maurice, F. Tuna, T. Mallah. *Inorg. Chem.*, **50**, 12045 (2011); (e) T. Birk, K.S. Pedersen, C.A. Thuesen, T. Weyhermüller, M. Schau-Magnussen, S. Piligkos, H. Weihe, S. Mossin, M. Evangelisti, J. Bendix. *Inorg. Chem.*, **51**, 5435 (2012); (f) J. Dreiser, K.S. Pedersen, C. Piamonteze, S. Rusponi, Z. Salman, M.E. Ali, M. Schau-Magnussen, C.A. Thuesen, S. Piligkos, H. Weihe, H. Mutka, O. Waldmann, P. Oppeneer, J. Bendix, F. Nolting, H. Brune. *Chem. Sci.*, **3**, 1024 (2012); (g) D.L. Reger, A.E. Pascui, M.D. Smith, J. Jezierska, A. Ozarowski. *Inorg. Chem.*, **51**, 7966 (2012); (h) R.K.B. Devi, S.P. Devi, R.K.B. Singh, R.K.H. Singh, T. Swu, W.R. Devi, C.H.B. Singh. *J. Coord. Chem.*, **67**, 891 (2014); (i) S.A. Khan, A. Noor, R. Kempe, H. Subhan, A. Shah, E. Khan. *J. Coord. Chem.*, **67**, 2425 (2014). doi: 10.1080/00958972.2014.938066.
- [14] S. Jamali, D. Milić, R. Kia, Z. Mazloomi, H. Abdolahi. *Dalton Trans.*, **40**, 9362 (2011).
- [15] (a) P. Bag, S. Dutta, P. Biswas, S.K. Maji, U. Flörke, K. Nag. *Dalton Trans.*, **41**, 3414 (2012); (b) I.A. Gass, B. Moubaraki, S.K. Langley, S.R. Batten, K.S. Murray. *Chem. Commun.*, **48**, 2089 (2012); (c) Y.-N. Guo, X.-H. Chen, S. Xue, J. Tang. *Inorg. Chem.*, **51**, 4035 (2012); (d) D.E. Janzen, M.E. Botros, D.G. VanDerveer, G.J. Grant. *Dalton Trans.*, 5316 (2007); (e) H. Ke, L. Zhao, G.-F. Xu, Y.-N. Guo, J. Tang, X.-Y. Zhang, H.-J. Zhang. *Dalton Trans.*, 10609 (2009); (f) S.K. Langley, B. Moubaraki, K.S. Murray. *Inorg. Chem.*, **51**, 3947

- (2012); (g) X.-L. Tang, W.-H. Wang, W. Dou, J. Jiang, W.-S. Liu, W.-W. Qin, G.-L. Zhang, H.-R. Zhang, K.-B. Yu, L.-M. Zheng. *Angew. Chem. Int. Ed.*, **48**, 3499 (2009); (h) H. Tian, L. Zhao, Y.-N. Guo, Y. Guo, J. Tang, Z. Liu. *Chem. Commun.*, **48**, 708 (2012); (i) L. Wang, Y. Li, Y. Peng, Z. Liang, J. Yu, R. Xu. *Dalton Trans.*, **41**, 6242 (2012); (j) J.-Y. Xu, H.-B. Song, G.-F. Xu, X. Qiao, S.-P. Yan, D.-Z. Liao, Y. Journaux, J. Cano. *Chem. Commun.*, **48**, 1015 (2012); (k) J. Vallejo, J. Cano, I. Castro, M. Julve, F. Lloret, O. Fabelo, L. Cañadillas-Delgado, E. Pardo. *Chem. Commun.*, **48**, 7726 (2012); (l) A.M. Garcia-Deibe, C. Portela-García, M. Fondo, A.J. Mota, J. Sanmartín-Matalobos. *Chem. Commun.*, **48**, 9915 (2012).
- [16] (a) P.C. Andrews, T. Beck, C.M. Forsyth, B.H. Fraser, P.C. Junk, M. Massi, P.W. Roesky. *Dalton Trans.*, 5651 (2007); (b) L. Zhao, S. Xue, J. Tang. *Inorg. Chem.*, **51**, 5994 (2012).
- [17] A.S.R. Chesman, D.R. Turner, B. Moubaraki, K.S. Murray, G.B. Deacon, S.R. Batten. *Chem. Eur. J.*, **15**, 5203 (2009).
- [18] (a) K. Xiong, X. Wang, F. Jiang, Y. Gai, W. Xu, K. Su, X. Li, D. Yuan, M. Hong. *Chem. Commun.*, **48**, 7456 (2012); (b) A.S.R. Chesman, D.R. Turner, B. Moubaraki, K.S. Murray, G.B. Deacon, S.R. Batten. *Dalton Trans.*, **41**, 10903 (2012).
- [19] K.S. Jeong, Y.S. Kim, Y.J. Kim, E. Lee, J.H. Yoon, W.H. Park, Y.W. Park, S.-J. Jeon, Z.H. Kim, J. Kim, N. Jeong. *Angew. Chem. Int. Ed.*, **45**, 8134 (2006).
- [20] R. Sen, D.K. Hazra, M. Mukherjee, S. Koner. *Eur. J. Inorg. Chem.*, 2826 (2011).
- [21] (a) J.-B. Peng, Q.-C. Zhang, X.-J. Kong, Y.-Z. Zheng, Y.-P. Ren, L.-S. Long, R.-B. Huang, L.-S. Zheng, Z. Zheng. *J. Am. Chem. Soc.*, **134**, 3314 (2012); (b) S. Sakamoto, T. Fujinami, K. Nishi, N. Matsumoto, N. Mochida, T. Ishida, Y. Sunatsuki, N. Re. *Inorg. Chem.*, **52**, 7218 (2013); (c) K. Ehama, Y. Ohmichi, S. Sakamoto, T. Fujinami, N. Matsumoto, N. Mochida, T. Ishida, Y. Sunatsuki, M. Tsuchimoto, N. Re. *Inorg. Chem.*, **52**, 12828 (2013); (d) T.N. Hooper, R. Inglis, M.A. Palacios, G.S. Nichol, M.B. Pitak, S.J. Coles, G. Lorusso, M. Evangelisti, E.K. Brechin. *Chem. Commun.*, **50**, 3498 (2014).
- [22] R. McLellan, J. Rezé, S.M. Taylor, R.D. McIntosh, E.K. Brechin, S.J. Dalgarno. *Chem. Commun.*, **50**, 2202 (2014).
- [23] C. Bazzicalupi, A. Bencini, A. Bencini, A. Bianchi, F. Corana, V. Fusi, C. Giorgi, P. Paoli, P. Paoletti, B. Valtancoli, C. Zanchini. *Inorg. Chem.*, **35**, 5540 (1996).
- [24] (a) J. Notni, S. Schenk, H. Görls, H. Breitzke, E. Anders. *Inorg. Chem.*, **47**, 1382 (2008); (b) X. Liu, P. Du, R. Cao. *Nat. Commun.*, **4**, 2375 (2013).
- [25] C.-P. Li, M. Du. *Chem. Commun.*, **47**, 5958 (2011).
- [26] H. Ke, P. Gamez, L. Zhao, G.-F. Xu, S. Xue, J. Tang. *Inorg. Chem.*, **49**, 7549 (2010).
- [27] (a) H. Ke, L. Zhao, Y. Guo, J. Tang. *Inorg. Chem.*, **51**, 2699 (2012); (b) K.C. Mondal, A. Sundt, Y. Lan, G.E. Kostakis, O. Waldmann, L. Ungur, L.F. Chibotaru, C.E. Anson, A.K. Powell. *Angew. Chem. Int. Ed.*, **51**, 7550 (2012); (c) I. Nemeč, M. Machata, R. Herchel, R. Boča, Z. Trávníček. *Dalton Trans.*, **41**, 14603 (2012); (d) H. Ke, W. Zhu, S. Zhang, G. Xie, S. Chen. *Polyhedron*, **87**, 109 (2015).
- [28] C. Pettinari, F. Marchetti, R. Pettinari, D. Martini, A. Drozdov, S. Troyanov. *Inorg. Chim. Acta*, **325**, 103 (2001).
- [29] G.M. Sheldrick. *Acta Crystallogr., Sect. A: Found. Crystallogr.*, **64**, 112 (2008).
- [30] T.N. Hooper, J. Schnack, S. Piligkos, M. Evangelisti, E.K. Brechin. *Angew. Chem. Int. Ed.*, **51**, 4633 (2012).
- [31] (a) X.-J. Kong, L.-S. Long, R.-B. Huang, L.-S. Zheng, T.D. Harris, Z. Zheng. *Chem. Commun.*, 4354 (2009); (b) Y.-Z. Zheng, M. Evangelisti, R.E.P. Winpenny. *Angew. Chem. Int. Ed.*, **50**, 3692 (2011); (c) C. Papatriantafyllopoulou, T.C. Stamatatos, C.G. Efthymiou, L. Cunha-Silva, F.A.A. Paz, S.P. Perlepes, G. Christou. *Inorg. Chem.*, **49**, 9743 (2010); (d) J.-B. Peng, Q.-C. Zhang, X.-J. Kong, Y.-P. Ren, L.-S. Long, R.-B. Huang, L.-S. Zheng, Z. Zheng. *Angew. Chem. Int. Ed.*, **50**, 10649 (2011).
- [32] J.J. Borrás-Almenar, J.M. Clemente-Juan, E. Coronado, B.S. Tsukerblat. *Inorg. Chem.*, **38**, 6081 (1999).
- [33] A. Buchholz, A.O. Eseola, W. Plass. *C. R. Chim.*, **15**, 929 (2012).
- [34] A. Chakraborty, B.K. Ghosh, J. Ribas-Arino, J. Ribas, T.K. Maji. *Inorg. Chem.*, **51**, 6440 (2012).
- [35] (a) G. Cucinotta, M. Perfetti, J. Luzon, M. Etienne, P.-E. Car, A. Caneschi, G. Calvez, K. Bernot, R. Sessoli. *Angew. Chem. Int. Ed.*, **51**, 1606 (2012); (b) F. Habib, J. Long, P.-H. Lin, I. Korobkov, L. Ungur, W. Wernsdorfer, L.F. Chibotaru, M. Murugesu. *Chem. Sci.*, **3**, 2158 (2012).
- [36] Y. Song, F. Luo, M. Luo, Z. Liao, G. Sun, X. Tian, Y. Zhu, Z.-J. Yuan, S. Liu, W. Xu, X. Feng. *Chem. Commun.*, **48**, 1006 (2012).
- [37] (a) S.-Y. Lin, Y.-N. Guo, Y. Guo, L. Zhao, P. Zhang, H. Ke, J. Tang. *Chem. Commun.*, **48**, 6924 (2012); (b) Y.-Z. Zheng, Y. Lan, C.E. Anson, A.K. Powell. *Inorg. Chem.*, **47**, 10813 (2008).
- [38] K. Suzuki, R. Sato, N. Mizuno. *Chem. Sci.*, **4**, 596 (2013).
- [39] G.-J. Chen, C.-Y. Gao, J.-L. Tian, J. Tang, W. Gu, X. Liu, S.-P. Yan, D.-Z. Liao, P. Cheng. *Dalton Trans.*, **40**, 5579 (2011).